

# CrystEngComm

Accepted Manuscript



This is an *Accepted Manuscript*, which has been through the Royal Society of Chemistry peer review process and has been accepted for publication.

*Accepted Manuscripts* are published online shortly after acceptance, before technical editing, formatting and proof reading. Using this free service, authors can make their results available to the community, in citable form, before we publish the edited article. We will replace this *Accepted Manuscript* with the edited and formatted *Advance Article* as soon as it is available.

You can find more information about *Accepted Manuscripts* in the [Information for Authors](#).

Please note that technical editing may introduce minor changes to the text and/or graphics, which may alter content. The journal's standard [Terms & Conditions](#) and the [Ethical guidelines](#) still apply. In no event shall the Royal Society of Chemistry be held responsible for any errors or omissions in this *Accepted Manuscript* or any consequences arising from the use of any information it contains.



Journal Name

ARTICLE

# Direct growth of ZnO nanowire arrays on UV-irradiated graphene

Received 00th January 20xx,  
Accepted 00th January 20xx

Ming-Yen Lu<sup>a,b,\*</sup>, Yen-Min Ruan<sup>a,b</sup>, Cheng-Yao Chiu<sup>a,b</sup>, Ya-Ping Hsieh<sup>a</sup>, and Ming-Pei Lu<sup>c</sup>

DOI: 10.1039/x0xx00000x

[www.rsc.org/](http://www.rsc.org/)

In this study, we investigated the effect of UV irradiation of graphene on the hydrothermal growth of ZnO nanowires (NWs). We found that the density of ZnO NWs varied with respect to the UV irradiation time, with the highest density of ZnO NWs being achieved on a graphene surface that had been irradiated for 10 min. Transmission electron microscopy revealed that the ZnO NWs grew vertically on the graphene. The hydrophobicity of the graphene decreased after UV irradiation, enhancing the seeding and hydrothermal growth of ZnO NWs. Raman spectroscopic analysis revealed that UV irradiation of the graphene produced defects, which served as trapping centers during the seeding process. When UV irradiation was applied for more than 10 min, the number of carbon atoms with dangling bonds decreased, thereby decreasing the resulting density of ZnO NWs on the graphene. This facile strategy for growing uniform ZnO NWs on chemically inert graphene after UV irradiation should be suitable for adoption in other growth systems, potentially allowing the development of novel hybrid systems for use in electronic and optoelectronic devices.

## Introduction

Graphene, a two-dimensional atomic-layer material comprising  $sp^2$ -hybridized carbon atoms in the form of a honeycomb lattice, possesses extraordinary properties, including high carrier mobility<sup>1</sup>, high thermal conductivity<sup>2</sup>, high optical transmittance<sup>3</sup>, and excellent mechanical strength<sup>4</sup>. Accordingly, graphene is a promising material for use in many diverse applications, including electronic devices, sensors<sup>5, 6</sup>, and energy devices<sup>7</sup>. Interestingly, the introduction of graphene can enhance the performance of supercapacitors<sup>8</sup>, fuel cells<sup>9</sup>, and solar cells<sup>10</sup>. Because of its transparency, conduction, and flexibility, graphene has potential use as a substrate for flexible electronic and optoelectronic devices.

Hybrid material systems arising from the direct growth of semiconductor nanowires (NWs) on graphene substrates have drawn much attention because they allow the preparation of various transparent and flexible devices, including light-emitting diodes<sup>11</sup>, sensors<sup>12, 13</sup>, catalysts<sup>14-16</sup>, supercapacitors<sup>17</sup>, photodetectors<sup>18</sup>, and energy devices<sup>19</sup>. The absence of defects on its surface, however, makes graphene chemically inert,

complicating the large-scale nucleation or seeding on graphene surfaces for epitaxial growth. Several growth strategies have been demonstrated recently<sup>20, 21</sup>. Taking the growth of ZnO NWs on graphene as an example, Yi and co-workers reported that ZnO NWs could be grown vertically on a graphene surface through catalyst-free metalorganic vapor epitaxy<sup>22</sup>, with the density of NWs being much higher at the step edges of the graphene surface because of the larger number of the structural defects at these locations. The hydrothermal growth of ZnO NWs on graphene has also been demonstrated<sup>23</sup>, but with the density of the resulting ZnO NW arrays on graphene remaining low. Because defects on the graphene surface can be used as nucleation sites or molecular trapping centers for material growth, attempts have been made to modulate the number of defects on graphene surfaces using ion bombardment<sup>24</sup>, plasma treatment<sup>25</sup> and UV irradiation<sup>26</sup>; accordingly, several groups have not only increased the density but also controlled the sites of growth of ZnO NWs on graphene surfaces<sup>23, 27, 28</sup>. Nevertheless, the factors influencing the hydrothermal growth of ZnO NWs on graphene surfaces have not previously been investigated systematically. In this paper, we report the successful growth of uniformly distributed ZnO NWs on graphene after UV irradiation. The hydrophobicity and the defect density of the graphene both changed upon applying such an irradiation process. Herein, we discuss the correlations between the ZnO NW density and the hydrophobicity and defect density of the graphene.

## Experimental details

<sup>a</sup> Graduate Institute of Opto-Mechatronics, National Chung Cheng University, Chia-Yi 62102, Taiwan. E-mail: mylu@ccu.edu.tw

<sup>b</sup> Advanced Institute of Manufacturing with High-Tech Innovations, National Chung Cheng University, Chia-Yi 62102, Taiwan.

<sup>c</sup> National Nano Device Laboratories, Hsinchu 300, Taiwan.

† Footnotes relating to the title and/or authors should appear here.

Electronic Supplementary Information (ESI) available: [details of any supplementary information available should be included here]. See DOI: 10.1039/x0xx00000x

ZnO NWs were grown on graphene using the hydrothermal method. First, chemical vapor deposition (CVD)-grown graphene was transferred onto a supporting SiO<sub>2</sub>/Si substrate (the synthesis and transfer of graphene have been described previously)<sup>29</sup>. Prior to the hydrothermal growth of the ZnO NWs, the graphene was illuminated under 254-nm UV light in the sealed box for various durations, with the power density ranging from 1 to 4 mW/cm<sup>2</sup> (it was set at 3 mW/cm<sup>2</sup> in experiments related to studying the influence of UV irradiation of graphene on ZnO NW growth). Subsequently, 20 mM zinc acetate [Zn(CH<sub>3</sub>COO)<sub>2</sub>·2H<sub>2</sub>O] in EtOH was spun onto the samples, followed by oxidation at 350 °C for 30 min to form ZnO seeds. The samples were then immersed into a growth solution comprising equal concentrations (40 mM) of zinc nitrate hexahydrate [Zn(NO<sub>3</sub>)<sub>2</sub>·6H<sub>2</sub>O, 99.0%], hexamethylenetetramine (C<sub>6</sub>H<sub>12</sub>N<sub>4</sub>, HMTA, 99.0%), and 10 mM polyethylenimine (PEI). The solution was heated at 90 °C for 24 h for growth of the ZnO NWs. The samples were then rinsed with deionized water and dried under N<sub>2</sub>. The morphologies and crystal structures of the samples were investigated using field-emission scanning electron microscopy (FESEM, Hitachi S-4800) and transmission electron microscopy (TEM, JEOL JEM-ARM200F). Their wetting properties were investigated using contact angle measurements. Raman spectroscopy was used to evaluate the quality of the graphene.

## Results and discussion

Because graphene surfaces typically lack defects, they can be regarded as chemically stable materials that cannot readily undergo nucleation or molecular/ion trapping. External treatment (e.g., UV irradiation, plasma bombardment), however, can damage the sp<sup>2</sup>-hybridized C–C bonds of graphene, thereby generating defects. In this study, we applied UV irradiation to form defects that could be used as trapping centers for subsequent ZnO NW growth. The graphene substrates were spin-coated with seeds prior to the growth. Because the ZnO NWs were not grown vertically on the graphene, tilted-view SEM images provided a clearer picture of the evolution of the ZnO NW density between samples. Figs. 1a–e present 45°-tilted SEM images of ZnO NWs grown on pristine and UV-irradiated (for 5, 10, 15, and 20 min) graphene substrates, respectively; Fig. S1 provides corresponding top-view SEM images. The ZnO NWs that grew on the pristine graphene were loosely distributed over the sample at a density of  $4.67 \times 10^4/\text{mm}^2$ . Fig. 1f reveals that the NW densities varied with respect to the UV irradiation time. Upon increasing the irradiation time to 10 min, the NW density increased to a maximum of  $5.75 \times 10^5/\text{mm}^2$ —a density approximately 10 times higher than that on the pristine graphene. Further increases in the UV irradiation time decreased the NW density on the graphene substrate. We attribute the low density of ZnO NWs on the pristine graphene to the absence of surface defects, which suppressed the deposition of Zn ions during the seeding process. UV irradiation damaged the sp<sup>2</sup>-hybridized C atoms of graphene, thereby forming more trapping centers for seed

deposition. The average lengths and diameters of the ZnO NWs on the various samples ranged from 7 to 22 μm and from 400 to 1260 nm, respectively. Fig. 1g reveals that the length and diameter distributions of the ZnO NWs grown on the graphene surfaces exhibited a converse tendency with respect to the number of NWs, with relatively small NW length/diameter distributions occurring for the 10-min UV-treated sample presenting the densest array of NWs. The ZnO NWs grown on the UV-irradiated graphene with Zn seeding were much more dense than those prepared without seeding (Fig. S2), implying that the defects on graphene behaved mostly as trapping centers for Zn ions, rather than as the nucleation sites for ZnO NW growth.

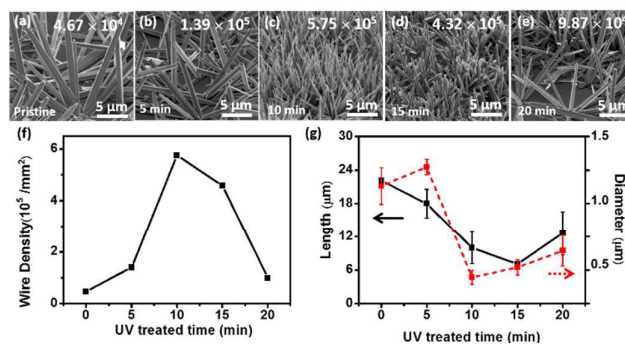


**Figure 1.** (a–e) 45°-Tilted FE-SEM images of ZnO NWs on graphene samples that had been UV-irradiated for (a) 0, (b) 5, (c), 10, (d) 15, and (e) 20 min. The numbers in each image are the numbers of NW per mm<sup>2</sup>. (f, g) Plots of (f) density and (g) average length and diameter of ZnO NWs grown on the various UV-irradiated graphene substrates.

We used TEM to investigate the crystal structures of the ZnO NWs grown on the graphene surfaces. The cross-sectional TEM image in Fig. 2a reveals that the ZnO NWs had grown vertically on the graphene substrate. The enlarged TEM image in Fig. 2b identifies native SiO<sub>2</sub> as the oxide on the Si supporting substrate, with the CVD-grown graphene appearing as a darkly contrasting atom-thin layer on top of the SiO<sub>2</sub>, serving as the substrate for subsequent growth of the ZnO NWs. Fig. 2c displays a high-resolution (HR) TEM image of the ZnO NW marked in Fig. 2b; the *d*-spacing of 0.52 nm corresponds to the (0001) plane of ZnO, confirming that the growth of the ZnO NWs occurred along the *c*-axis.

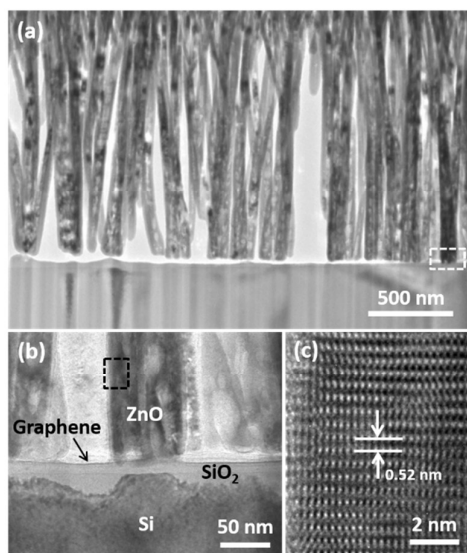


**Figure 2.** (a) Cross-sectional TEM image of ZnO NWs on a 10-min UV-irradiated graphene substrate. (b) Enlarged TEM image of the interfacial region of the graphene layer and the ZnO NWs. (c) HRTEM image of the ZnO NW marked in (b).

Because hydrothermal growth of ZnO NW arrays involves reactions performed in the liquid phase, the hydrophobicity of the graphene surface should be taken into account. Fig. 3 displays the contact angles measured to investigate the surface conditions of the graphene substrates after UV irradiation for various durations; the insets present corresponding optical images of water droplets on the surfaces. The contact angles of the pristine and UV-irradiated (for 5, 10, 15, and 20 min) graphene surfaces were 88.1, 87.0, 81.0, 79.4, and 74.1°, respectively. The hydrophobicity transitions of graphene surfaces arise from the dissociative adsorption of  $\text{H}_2\text{O}$ <sup>30</sup>. The hydrophilic graphene surfaces were more favorable for seeding and for ZnO hydrothermal growth.

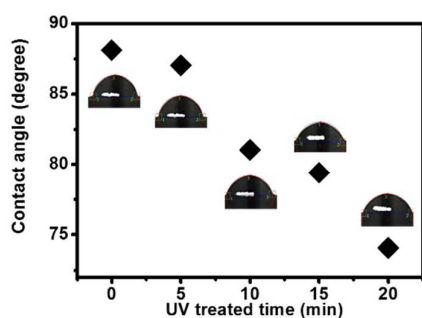


**Figure 3.** Contact angles of graphene samples that had been irradiated for different periods of time.

The UV radiation process not only affects the hydrophobicity of graphene surfaces but also generates defects on those surfaces<sup>31,32</sup>. The OM image of pristine CVD-grown graphene on the  $\text{SiO}_2$  substrate reveals (Fig. S3) that the substrate was mainly covered with single-layer graphene, with less than 10% of the sample area

being multilayer graphene; our initial investigation indicated that the value of the ratio  $I_{2D}/I_G$  of CVD-graphene was approximately 2.77, implying that the graphene existed in a single layer (Fig. S4), and, therefore, our single-layer graphene had a thickness of approximately 0.35 nm<sup>33</sup>. We recorded Raman spectra to characterize the crystal quality of our graphene samples after UV irradiation for various periods of time. Power-dependence investigations revealed that UV light at a power density of 3 mW/cm<sup>2</sup> had the most significant effect on defect formation on graphene (Fig. S5); thus, we used UV light of such power density when evaluating the quality of graphene after UV irradiation for various periods of time. Fig. 4a reveals that all of the samples exhibited three distinguishing peaks at 1360, 1580, and 2700 cm<sup>-1</sup>, corresponding to the D-, G-, and 2D-bands, respectively. The intensity ratio of the D- and G-bands ( $I_D/I_G$ ) is commonly used to evaluate the defect densities of graphene samples<sup>34</sup>. In this study, C atoms with dangling bonds formed from the transfer process and from the UV irradiation were the dominant defects; Fig. 4b presents a plot of the values of  $I_D/I_G$  of our graphene samples after irradiation for various durations. Upon increasing the UV irradiation time up to 10 min, the value of  $I_D/I_G$  increased, implying that the defect density increased accordingly. Interestingly, UV irradiation times of greater than 10 min decreased the  $I_D/I_G$  ratio thereafter. The distinct behavior of the  $I_D/I_G$  ratios in the Raman spectra can be explained by the formation of defects after UV irradiation: ozone was produced by UV light irradiating the air, with defects on graphene being generated after ozone bombardment<sup>29,32</sup>.

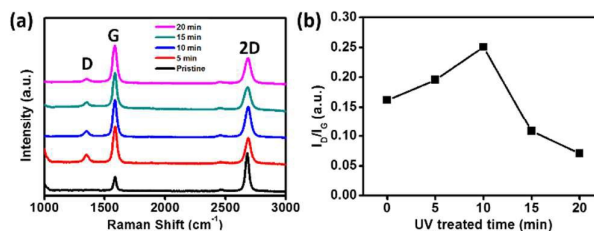


**Figure 4.** (a) Raman spectra and (b) plots of  $I_D/I_G$  ratios of pristine and UV-irradiated graphene samples.

To further comprehend the variations in the  $I_D/I_G$  ratios of graphene after different UV irradiation times, we used the film-induced frustrated etching method to examine the changes in the structural defects<sup>35</sup>. After UV irradiation, the samples of graphene on Cu foil were dipped into Cu etchant for 10 s; the etchant could penetrate the graphene via its structural defects to form etching pits on the Cu foil, with each etching pit being regarded as a structural defect. Fig. S6a - S6e present OM images of samples prepared without and with UV irradiation for 5 min, 10 min, 15 min, and 20 min, respectively. The dark dots are the etching pits on the Cu surface. Small pits were distributed on the Cu surface of the non-irradiated sample, but denser and larger etching pits appeared on the UV-irradiated samples. These differences imply that UV irradiation generated structural defects on the graphene, with the

size of the defects increasing upon increasing the irradiation time. Fig. 5 presents schematic representations of how we believe our graphene surfaces existed after UV irradiation for up to 20 min. Some imperfections were present in the pristine graphene (Fig. 5a), as defects formed during the CVD growth and transfer processes. UV light could then be used to engineer the defect density. In the early stages (up to 5 min) of UV irradiation, the graphene's  $sp^2$ -hybridized carbon network was damaged, with the density of carbon atoms with dangling bonds increasing over time (Fig. 5b); consequently, the  $I_D/I_G$  ratio increased. The  $I_D/I_G$  ratio reached its highest value after exposure for 10 min (Fig. 5c). The UV irradiation not only generated structural defects but also formed small-sized pits on the graphene surface. For the graphene that had been subjected to UV irradiation for a longer period of time (15 or 20 min), the pits become larger, possibly aggregating with adjacent pits to form big pits on the surface; meanwhile, the number of dangling bonds decreased, with the  $I_D/I_G$  ratios decreasing accordingly (Figs. 5d and 5e, respectively). Because carbon atoms with dangling bonds in the graphene served as trapping centers for the Zn ions during the seeding process, the trend in the variation in the  $I_D/I_G$  ratio was similar to that for the density of the ZnO NWs grown on the graphene surfaces with respect to the UV irradiation time.

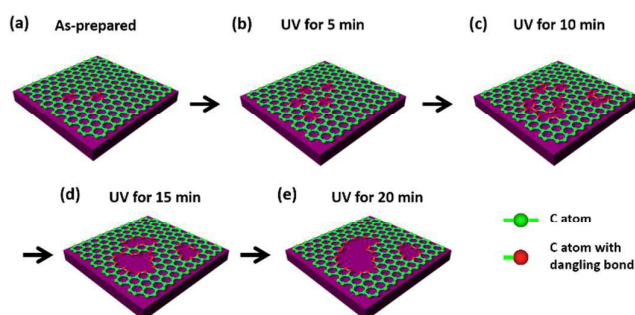


**Figure 5.** Schematic representation of the structure of a graphene sample after UV irradiation for various periods of time.

## Conclusions

We have examined the direct hydrothermal growth of ZnO NW arrays on UV-irradiated graphene. The density of ZnO NWs varied with respect to the irradiation time, reaching its maximum of  $5.75 \times 10^5/\text{mm}^2$  on the graphene that had been UV-irradiated for 10 min. HRTEM revealed that the ZnO NWs had grown vertically on the graphene surface. Moreover, the contact angles of the graphene surfaces revealed a transition from hydrophobic to hydrophilic after UV irradiation, with the resulting hydrophilic graphene surfaces being favorable for seeding and ZnO hydrothermal growth. UV irradiation generated defects on the graphene; from an investigation of Raman spectra, the level of defects, as characterized by the  $I_D/I_G$  ratio, increased upon increasing the UV irradiation time, reaching its highest value after treatment for 10 min. The  $I_D/I_G$  ratio decreased thereafter, implying that the number of carbon atoms with dangling bonds decreased. Most importantly, the defects in the graphene could act as trap centers for Zn ions during the seeding process; increasing the number of defects

increased the content of Zn ions trapped on the graphene, thereby increasing the density of subsequent ZnO NWs. This facile strategy of using UV exposure to affect the growth of uniform and dense ZnO NWs on chemically stable graphene should be adaptable to other growth systems—a potentially profitable exercise for developing novel hybrid materials for use in electronic and optoelectronic devices.

## Acknowledgement

We thank the Ministry of Science and Technology in Taiwan (MOST 103-2221-E-194 -050 -MY2) for financial support.

## Notes and references

1. Y. B. Zhang, Y. W. Tan, H. L. Stormer and P. Kim, *Nature*, 2005, **438**, 201-204.
2. A. A. Balandin, S. Ghosh, W. Z. Bao, I. Calizo, D. Teweldebrhan, F. Miao and C. N. Lau, *Nano Lett.*, 2008, **8**, 902-907.
3. C. M. Weber, D. M. Eisele, J. P. Rabe, Y. Y. Liang, X. L. Feng, L. J. Zhi, K. Mullen, J. L. Lyon, R. Williams, D. A. V. Bout and K. J. Stevenson, *Small*, 2010, **6**, 184-189.
4. C. Lee, X. D. Wei, J. W. Kysar and J. Hone, *Science*, 2008, **321**, 385-388.
5. F. Schedin, A. K. Geim, S. V. Morozov, E. W. Hill, P. Blake, M. I. Katsnelson and K. S. Novoselov, *Nat. Mater.*, 2007, **6**, 652-655.
6. Y. J. Wang, F. M. Wang and J. He, *Nanoscale*, 2013, **5**, 11291-11297.
7. X. L. Wang and G. Q. Shi, *Energy Environ. Sci.*, 2015, **8**, 790-823.
8. G. H. Yu, L. B. Hu, N. A. Liu, H. L. Wang, M. Vosgueritchian, Y. Yang, Y. Cui and Z. A. Bao, *Nano Lett.*, 2011, **11**, 4438-4442.
9. H. Y. Yuan and Z. He, *Nanoscale*, 2015, **7**, 7022-7029.
10. R. Bajpai, S. Roy, P. Kumar, P. Bajpai, N. Kulshrestha, J. Rafiee, N. Koratkar and D. S. Misra, *ACS Appl. Mater. Interfaces*, 2011, **3**, 3884-3889.
11. K. Chung, C. H. Lee and G. C. Yi, *Science*, 2010, **330**, 655-657.
12. A. Pandikumar, G. T. S. How, T. P. See, F. S. Omar, S. Jayabal, K. Z. Kamali, N. Yusoff, A. Jamil, R. Ramaraj, S. A. John, H. N. Lim and N. M. Huang, *RSC Adv.*, 2014, **4**, 63296-63323.

13. C. S. Boland, U. Khan, C. Backes, A. O'Neill, J. McCauley, S. Duane, R. Shanker, Y. Liu, I. Jurewicz, A. B. Dalton and J. N. Coleman, *ACS Nano*, 2014, **8**, 8819-8830.
14. Y. J. Wang, X. Y. Zhan, F. M. Wang, Q. S. Wang, M. Safdar and J. He, *J. Mater. Chem. A*, 2014, **2**, 18413-18419.
15. X. X. Gao, J. Wang, J. L. Yu and H. B. Xu, *CrystEngComm*, 2015, **17**, 6328-6337.
16. Z. Chen, N. Zhang and Y. J. Xu, *CrystEngComm*, 2013, **15**, 3022-3030.
17. X. C. Dong, Y. F. Cao, J. Wang, M. B. Chan-Park, L. H. Wang, W. Huang and P. Chen, *RSC Adv.*, 2012, **2**, 4364-4369.
18. V. Q. Dang, T. Q. Trung, D. I. Kim, L. T. Duy, B. U. Hwang, D. W. Lee, B. Y. Kim, L. D. Toan and N. E. Lee, *Small*, 2015, **11**, 3054-3065.
19. D. Choi, M. Y. Choi, W. M. Choi, H. J. Shin, H. K. Park, J. S. Seo, J. Park, S. M. Yoon, S. J. Chae, Y. H. Lee, S. W. Kim, J. Y. Choi, S. Y. Lee and J. M. Kim, *Adv. Mater.*, 2010, **22**, 2187-2192.
20. Y. J. Hong and T. Fukui, *ACS Nano*, 2011, **5**, 7576-7584.
21. A. M. Munshi, D. L. Dheeraj, V. T. Fauske, D. C. Kim, A. T. J. van Helvoort, B. O. Fimland and H. Weman, *Nano Lett.*, 2012, **12**, 4570-4576.
22. W. I. Park, C. H. Lee, J. M. Lee, N. J. Kim and G. C. Yi, *Nanoscale*, 2011, **3**, 3522-3533.
23. Y. J. Kim, Hadiywarman, A. Yoon, M. Kim, G. C. Yi and C. Liu, *Nanotechnology*, 2011, **22**, 245603.
24. B. An, S. Fukuyama, K. Yokogawa and M. Yoshimura, *J. Appl. Phys.*, 2002, **92**, 2317-2322.
25. K. Thiyagarajan, A. Ananth, B. Saravanakumar, Y. S. Mok and S. J. Kim, *RSC Adv.*, 2015, **5**, 16821-16827.
26. G. Imamura and K. Saiki, *ACS Appl. Mater. Interfaces*, 2015, **7**, 2439-2443.
27. Y. J. Kim, H. Tukiman, C. H. Lee, S. S. Kim, J. Park, B. H. Sohn, M. Kim, G. C. Yi, R. Jung and C. Liu, *Curr. Appl. Phys.*, 2014, **14**, 269-274.
28. Y. J. Kim, H. Yoo, C. H. Lee, J. B. Park, H. Baek, M. Kim and G. C. Yi, *Adv. Mater.*, 2012, **24**, 5565-5569.
29. Y. P. Hsieh, M. Hofmann, K. W. Chang, J. G. Jhu, Y. Y. Li, K. Y. Chen, C. C. Yang, W. S. Chang and L. C. Chen, *ACS Nano*, 2014, **8**, 443-448.
30. Z. M. Xu, Z. M. Ao, D. W. Chu, A. Younis, C. M. Li and S. A. Li, *Sci Rep*, 2014, **4**, 6450.
31. F. Gunes, G. H. Han, H. J. Shin, S. Y. Lee, M. Jin, D. L. Duong, S. J. Chae, E. S. Kim, F. Yao, A. Benayad, J. Y. Choi and Y. H. Lee, *Nano*, 2011, **6**, 409-418.
32. A. Tracz, G. Wegner and J. P. Rabe, *Langmuir*, 2003, **19**, 6807-6812.
33. S. C. Xu, B. Y. Man, S. Z. Jiang, C. S. Chen, C. Yang, M. Liu, X. G. Gao, Z. C. Sun and C. Zhang, *CrystEngComm*, 2013, **15**, 1840-1844.
34. D. Y. Pan, J. C. Zhang, Z. Li and M. H. Wu, *Adv. Mater.*, 2010, **22**, 734-738.
35. M. Hofmann, Y. C. Shin, Y. P. Hsieh, M. S. Dresselhaus and J. Kong, *Nano Res*, 2012, **5**, 504-511.

The influences of UV light to graphene for ZnO nanowire growth were discussed

